

Article

Nanocomposites Based on Metal and Metal Sulfide Clusters Embedded in Polystyrene

Gianfranco Carotenuto ^{1,*}, Cinzia Giannini ², Dritan Siliqi ² and Luigi Nicolais ¹

¹ Istituto per i Materiali Compositi e Biomedici, CNR, Piazzale V. Tecchio, Napoli 80-80125, Italy; E-Mail: nicolais@unina.it (L.N.)

² Istituto di Cristallografia, CNR, Via G. Amendola, Bari 122/O-70126, Italy; E-Mails: cinzia.giannini@ic.cnr.it (C.G.); dritan.siliqi@ic.cnr.it (D.S.)

* Author to whom correspondence should be addressed; E-Mail: giancaro@unina.it.

Received: 9 July 2011 / Accepted: 10 August 2011 / Published: 22 August 2011

Abstract: Transition-metal alkane-thiolates (*i.e.*, organic salts with formula $Me(SR)_x$, where R is a linear aliphatic hydrocarbon group, $-C_nH_{2n+1}$) undergo a thermolysis reaction at moderately low temperatures (close to 200 °C), which produces metal atoms or metal sulfide species and an organic by-product, disulfide (RSSR) or thioether (RSR) molecules, respectively. Alkane-thiolates are non-polar chemical compounds that dissolve in most techno-polymers and the resulting solid solutions can be annealed to generate polymer-embedded metal or metal sulfide clusters. Here, the preparation of silver and gold clusters embedded into amorphous polystyrene by thermolysis of a dodecyl-thiolate precursor is described in detail. However, this chemical approach is quite universal and a large variety of polymer-embedded metals or metal sulfides could be similarly prepared.

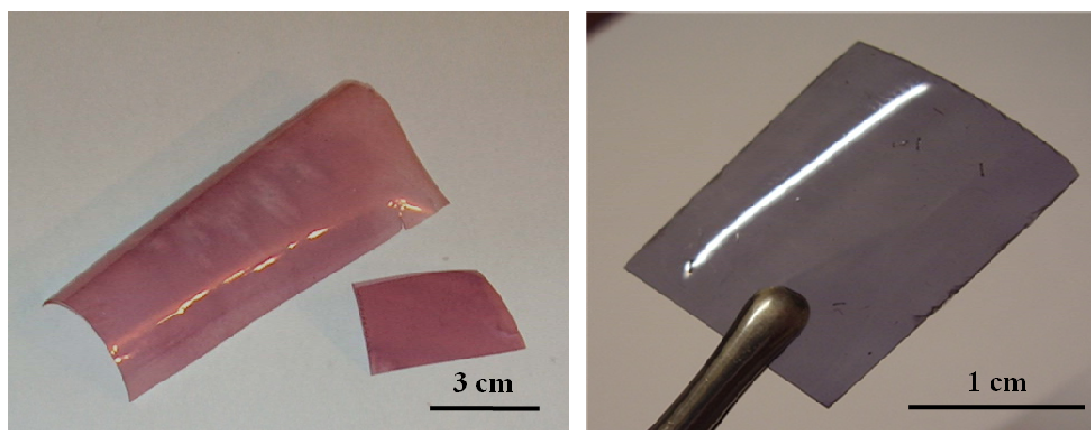
Keywords: metal clusters; thiolates; nanocomposites; polymer; optical properties

1. Introduction

New physical properties appear in a metallic phase when the size is reduced to a nanometric scale (for example, spherical particles with a diameter of only a few nanometers) [1,2]. Depending on the metal type, the nanoscopic particles can be colored (Au, Ag, Cu), fluorescent (Au, Ag), superparamagnetic (Co, Ni, Fe), melting at lower temperatures, *etc.* In addition, such new properties are strictly size-dependent and therefore they can be accurately tuned by simply changing the

morphology of the metallic phase (both size and shape) or making alloyed metal nanoparticles. The color of nanoscopic coin metals is due to the easy polarization of these small metal domains under visible light; such phenomenon is known as surface plasmon resonance (SPR) and may produce very strong optical extinctions in well-defined spectral ranges (see Figure 1). The electronic structure of a metal domain depends on the number of contained atoms (and therefore on the number of atomic orbitals which are combined together). As a result, the electronic configuration of a small metal cluster is very different from that of the corresponding bulk-metal, and may resemble that of organic molecules (the band structure of bulk-metal is replaced by discrete energy levels). As a consequence, fluorescence and other typical molecular properties appear in these nano-phases. Also thermodynamic properties are modified in nanoscopic metals because of the large surface free energy contribution (for example, the melting point is lowered). Chemical reactivity is increased and other physicochemical characteristics are modified (e.g., the catalytic activity of noble-metal is strongly increased). Nanoscopic semiconductor phases like metal sulfides (Me_xS_y) and other chalcogenides show anomalous behavior, such as a strong and tunable fluorescence.

Figure 1. Polystyrene films dyed by the surface plasmon resonance of gold nanoparticles. Depending on the average cluster size, films of different colors can be achieved (ruby-red, purple, and blue).



The novel properties of nanoscopic metal and sulfide phases can be used to functionalize optical plastics (*i.e.*, colorless amorphous polymers with a refractive index similar to glass, 1.5, e.g., polystyrene, poly(methyl methacrylate), polycarbonate, thermoplastic polyurethane, *etc.* [3–5]). Such polymer-embedded nanostructures can be easily handled and used for fabricating a number of optical devices exploitable for applications in different technological fields (linear optics, optoelectronics, magneto-optics, *etc.*). Optical plastics can be dyed, made magnetic or fluorescent without losing their transparency, and the resulting materials have great potential for functional applications. In addition, the nanostructures can be safely handled in a polymer-embedded form and aggregation, oxidation, and contamination by environmental molecules are prevented.

In order to investigate the technological potential of such nanostructured material class (metal/polymer and metal-sulfide/polymer nanocomposites), the availability of a general chemical route adequate to produce different combinations of polymers and atomic or molecular clusters should

be made available. At present, only a few preparative schemes have been developed [6], and these chemical approaches work only for some metal/polymer combinations.

Noble-metals, semimetals, and metal sulfides can be produced by thermal decomposition of alkane-thiolates at moderately low temperatures (close to 200 °C). The use of such reactions for the preparation of thioether and disulfide molecules is known in organic chemistry [7]. However the same chemical process has only occasionally been exploited to produce the inorganic phase (e.g., noble-metal coatings on ceramic substrates [8]). In the present work, the controlled thermolysis of alkane-thiolates dissolved in amorphous polystyrene has been used to generate polymer-embedded metals or metal sulfides of nanoscopic size. In particular, dodecyl-thiolates of gold, silver and other metals have been used because they derive from an odorless thiol (dodecyl-thiol) and produce non-volatile thermolysis by-products, as required to avoid film foaming during the annealing process.

2. Experimental

Dodecyl-thiolates of different metals (e.g., Au, Ag, Pd, Pt, Pb, Cd, Zn, *etc.*) were obtained by the following general preparative scheme based on the use of metal salts which are quite soluble in alcohol. A few milliliters of dodecanethiol (Aldrich, 98%) were dissolved in ethanol and added drop-wise and under stirring to a stoichiometric quantity of an alcoholic metal salt solution. During the reaction, the reactive system became a slurry because of thiolate precipitation, and reaction yields of close to 100% resulted because of the low metal thiolate solubility in alcohols. The reducing thiols can lower the oxidation number of the metallic ion before precipitation. In particular, with no change in the metal ion oxidation number (e.g., Cd²⁺, Pb²⁺, and Pd²⁺ ions) a prompt precipitation occurred, while precipitation was delayed when the oxidation state of the metal changed (e.g., Au-SR formation from Au³⁺ salt). The crystalline metal thiolates were separated by vacuum filtration and washed several times with acetone, then they were purified by dissolution in hot chloroform (50 °C), and precipitated again by adding of ethanol. In order to prepare thiolate-polymer solid solutions, the dry powder was dissolved in chloroform and mixed with a chloroform solution of amorphous polystyrene (PS, Aldrich, M_w = 90,000). Then, the system was cast onto a glass substrate (Petri dish) and solvent allowed to evaporate. To obtain nano-sized metal or metal sulfide dispersions, a thiolate content lower than 10 wt% was required. Isothermal annealing treatments were made by a laboratory hot-plate at a temperature of *ca.* 200 °C for a few minutes.

In the preparation of TEM specimens, the nanocomposite material was dissolved in chloroform and the solution added drop-wise to a Formovar covered copper grid. The dry films were then coated with graphite by sputtering. Such an approach is quite simple, however, differently from a solid sample slicing by cryo-ultramicrotome, artifacts in the sample topology can be introduced because of a possible cluster reorganization in the liquid dispersion. Transmission electron micrographs were obtained by using a Philips EM208S microscope, with an accelerating voltage of 100 kV. In the case of metal clusters characterized by surface plasmon absorption, the cluster formation was verified by UV-Vis spectroscopy. Optical spectra were recorded using a UV-Vis-NIR spectrophotometer (HP-8453 UV-Vis Spectrophotometer), equipped with a Peltier apparatus to control the sample temperature with an accuracy of 0.1 °C. The conclusions about the structure of nanoparticles were mainly based on analysis of thermolysis product. In particular, the thermogravimetric analysis

(TGA, TA-Instrument Mod.Q500) of nanocomposites and pure thiolate samples were carried out at 10 °C/min, under fluxing nitrogen.

The obtained polymer-embedded nano-crystals were characterized by X-ray Powder Diffraction (XPD). Data were collected with a D8 Discover-Bruker diffractometer equipped with a Goebel mirror for Cu radiation, an Eulerian cradle goniometer and a scintillation detector. The powder diffraction patterns were collected in the range 10–100° with a step size of 0.05°.

3. Results and Discussion

The microstructure of the obtained nanocomposite materials was imaged by transmission electron microscopy (TEM). Figure 2 shows the inner structure of a nanocomposite sample obtained by annealing an AuSC₁₂H₂₅/polystyrene solid solution for 5 min at 170 °C. In these nanocomposite films, the clusters were organized in form of large aggregates. Probably, the disulfide molecules produced as by-product of the annealing process are chemisorbed on the metal cluster surface, leading to thiol-derivatized clusters that interact with each other by interdigitation of thiolate chains [9]. The presence of thiolate on the cluster surface caused the nanoparticles to be close-packed and uniformly spaced. Such a special topology of nanocomposite films was not observed with all types of metal particles probably because thiolate molecules can be chemisorbed only on some types of metallic surfaces (e.g., Au, Ag, *etc.*). However, the method of preparation of samples for electron microscopy through dissolution of nanocomposites in solution provides information about the particle sizes but, of course, does not provide direct information about the stage of aggregation of particles in the solid materials just after the annealing treatment (instead, the topology observed in SEM micrographs surely results after material processing by solution casting).

When metals characterized by a surface plasmon absorption (e.g., gold and silver) were generated inside the polystyrene matrix by this technique, the nanocomposite films showed the characteristic color of the nano-sized metal (see Figure 3). In particular, polystyrene films containing silver thiolate (AgSC₁₂H₂₅) developed a yellow color during the annealing treatment which changed to brown when cooling the films down. The color variation was probably produced by a multiple-splitting of the silver surface plasmon absorption as a result of a decrease in the interparticle distance which causes interactions among particle dipoles. In other words, when silver nanoparticles are close enough to each other (as usually happens at temperatures lower than the thiolate coating melting point), the system showed a broad absorption band in the whole visible spectra; whereas, when particles are well-spaced (at temperatures higher than the thiolate coating melting point), the spectrum revealed just the tight surface plasmon absorption band of silver clusters located at 430 nm. Such thermochromic behavior of polystyrene films filled by silver clusters can have important applications in the sensor field. Gold-filled polystyrene films appeared ruby-red but they become blue after prolonged annealing treatments because of a significant growth of the metal nanoparticles.

Figure 2. TEM-micrographs of Au clusters embedded into amorphous polystyrene (the AuSC₁₂H₂₅/polystyrene solution was isothermally annealed for 5 min at 170 °C). Owing to the interdigitation and consequent co-crystallization of the thiol alkyl-chains coating the cluster surface, large cluster aggregates are present in this system.

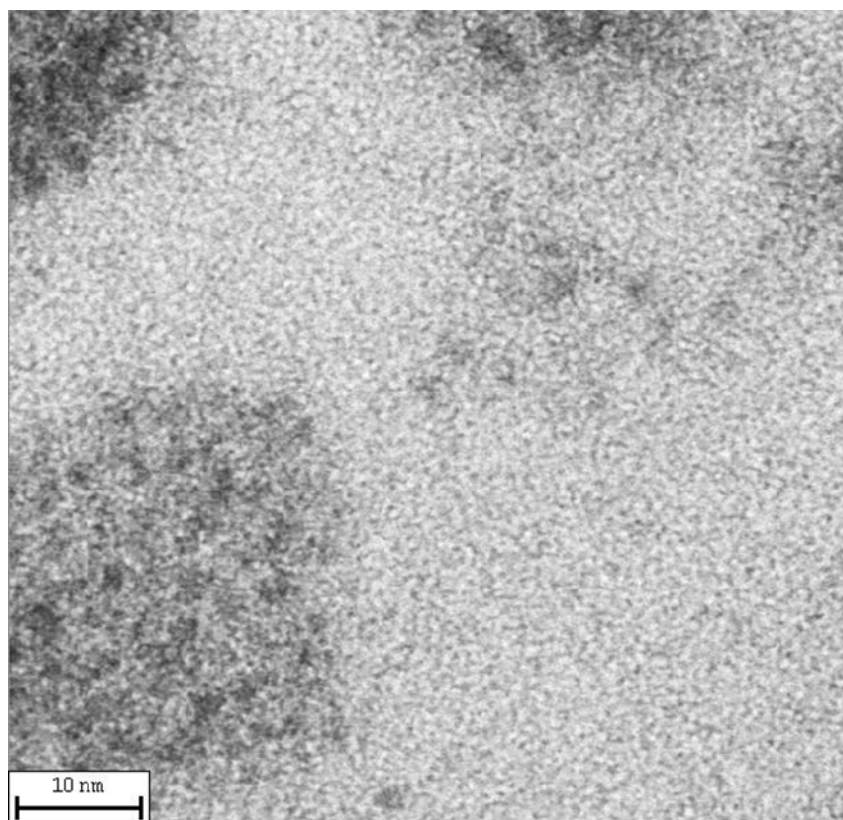
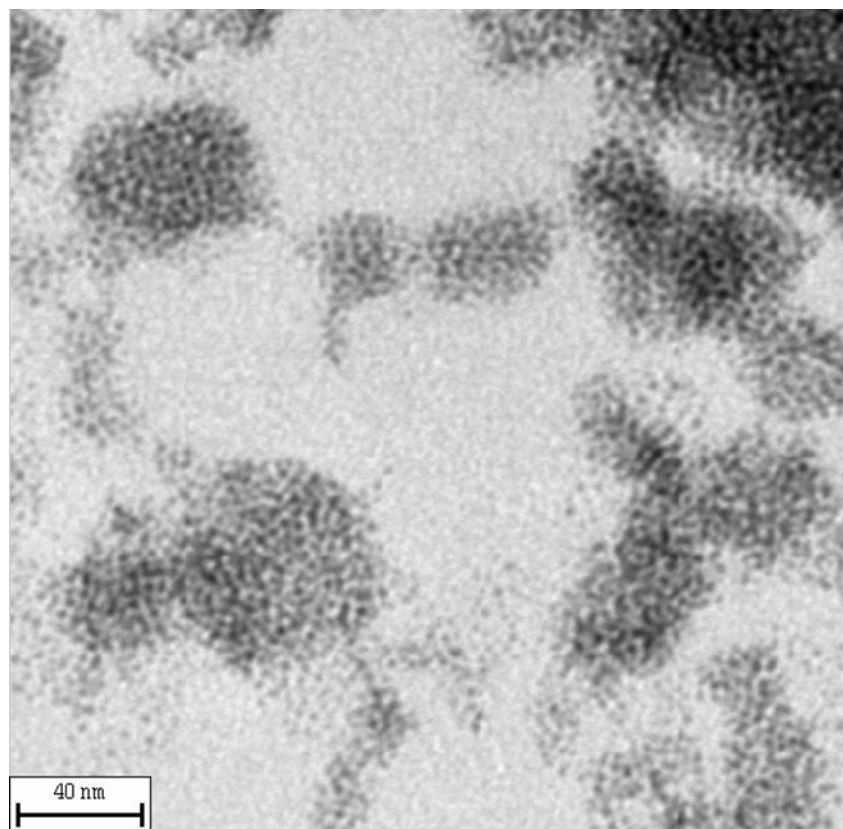
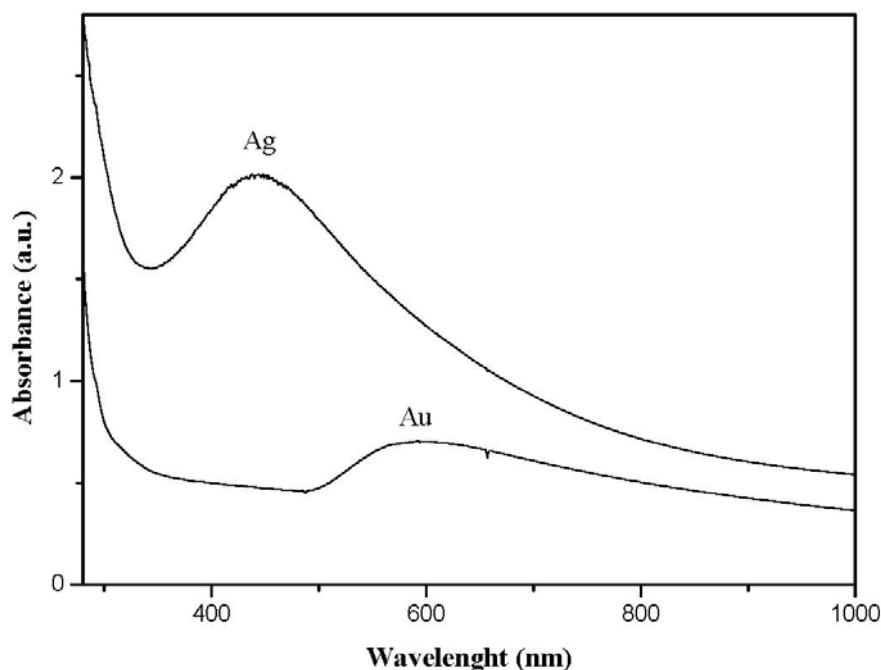


Figure 3. UV-Vis spectra of polystyrene-embedded gold and silver clusters. The characteristic surface plasmon absorptions of silver at 430 nm and of gold at 590 nm reveal the metal formation on a nano-sized scale.



The XPD patterns were collected on two samples: the first one consisted of a gold/polystyrene film obtained by thermal annealing of a gold dodecyl-thiolate solid solution at 200 °C, and the second sample was the same film after a dipping of 48 h in pure acetone. XPD data were analyzed by using a whole profile fitting Rietveld-based program, named FullProf [10]. A three-step procedure was followed:

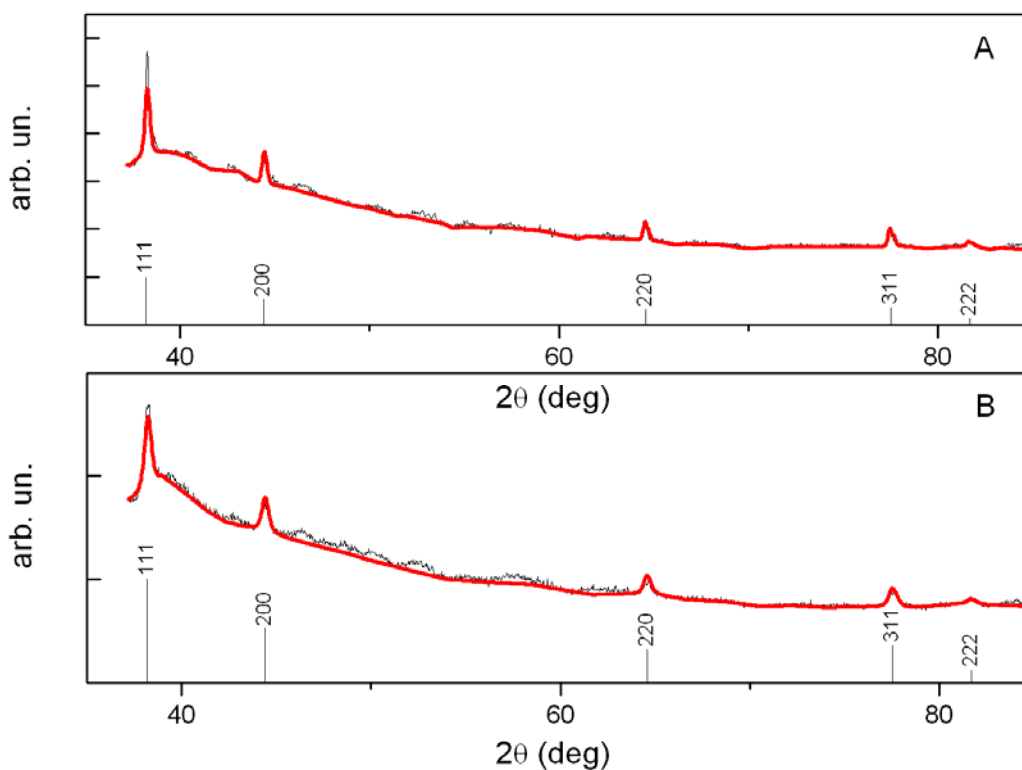
1. The instrumental resolution function (IRF) was evaluated by fitting the XPD pattern collected on a LaB6 NIST standard, measured in the same experimental conditions of the samples. The IRF file was provided separately to the program to refine the XPD patterns of the nanocrystals.
2. The crystal structure model used in the fits was Au
3. An isotropic peak broadening parameter of the diffraction pattern was refined with a phenomenological model based on a modified Scherrer formula. Another refinable parameter is the unit cell a value.

Two samples were used. The first one consisted of an as annealed Au/polystyrene film and the second was the same film after purification with acetone.

The refine cell parameter a is 4.088 Å and 4.0831 Å for the first and the second sample respectively. The average size of the nanoparticles is between 28–30 nm.

The results of the fits are shown in Figure 4(A) (for the first sample) and Figure 4(B) for the second sample, where the experimental pattern (black line) and the Rietveld best calculated profile (red line) are compared [Goodness of the Fit (GoF) is 3.1]. More sophisticated approaches based on total scattering methods are advisable at smaller particles size [11–13].

Figure 4. XRD diffractogram of gold clusters embedded in amorphous polystyrene before (A); and after (B) film dipping in pure acetone (the nanocomposite sample was obtained by isothermally annealing an AuSC₁₂H₂₅/polystyrene solution for 2 min at 200 °C).



Stoichiometric information on the thermolysis products was obtained by thermogravimetric analysis (TGA) of the pure thiolate compounds (see Figure 5). Thermolysis products and other experimental information for some thiolate compounds are given in Table 1.

Figure 5. TGA-thermograms of pure thiolate compounds: (A) gold dodecyl-thiolate; and (B) lead dodecyl-thiolate. The residual weight corresponds respectively to the metal (Au) and metal sulfide (PbS) percentage in the thiolate compound.

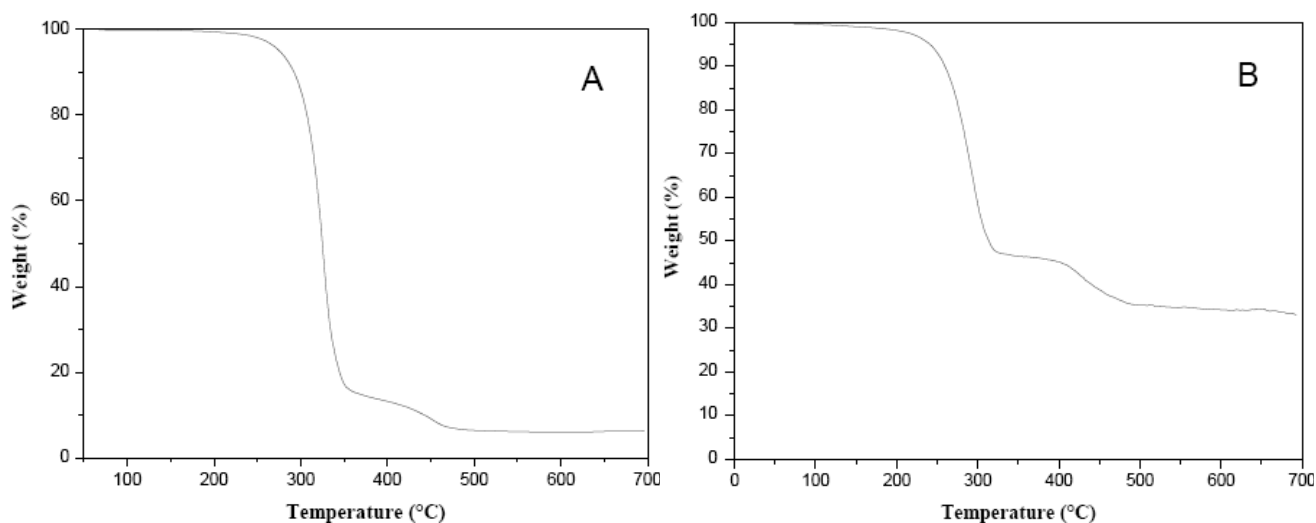
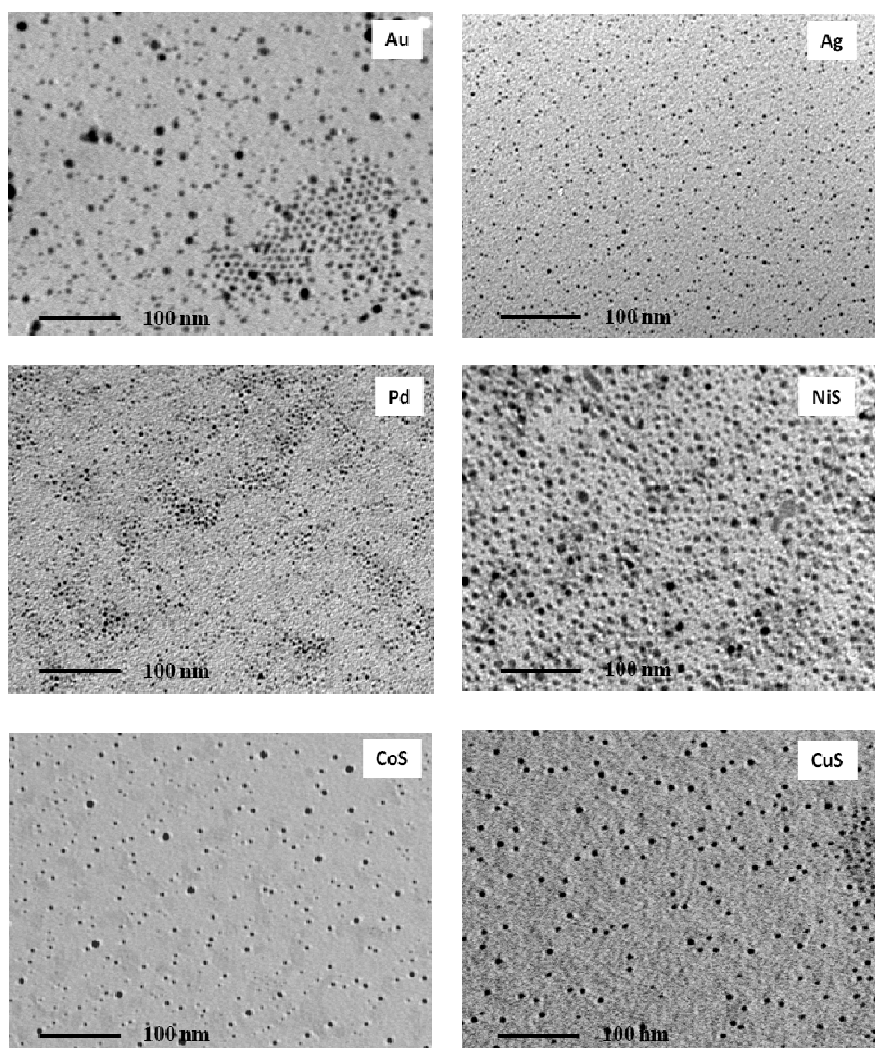


Figure 6. TEM-micrographs of different metal and metal sulfide clusters embedded into an amorphous polystyrene matrix, obtained by thermal decomposition of the corresponding metal-dodecylthiolate compounds [23–29].



Dodecylthiolates of transition metals are organic compounds very adequate as precursor for the generation of nano-sized metals or metal sulfides in molten thermoplastic polymers (see Figure 6). These compounds are of a non-polar nature because the ionic contribution to the Me-S bond is quite low, and consequently dissolution in non-polar organic media like techno-polymers and hydrophobic solvents (e.g., chloroform, ether, *etc.*) is possible. The use of dodecyl-thiolates (or heavier alkane-thiolates) is required to avoid nanocomposite film foaming during the annealing process caused by the volatile by-product of thermolysis reaction. Noble metal-sulfur bond energies are usually low ($200\text{--}300\text{ kJ mol}^{-1}$) [14] and dissociation may occur at temperatures close to $200\text{ }^{\circ}\text{C}$. However, these compounds are very stable at room temperature and can be handled/stored without special care. The thermal decomposition reaction occurs for alkane-thiolate of transition metals characterized by low electronegativity values (Cd, Zn, Pb, Cu, Co, *etc.*) according to the following reaction [15–19]:



However, noble-metals (Au, Ag, Pt, Pd, *etc.*) and most semi-metals (Sb) produce the metallic phase [20–22], according to the following reaction:



The temperature required for thermal degradation depends on the degradation mechanism and usually it is higher in the case of sulfide formation.

Table 1. Some characteristics of metal thiolates used for the nanocomposite film preparation.

| Thiolate | Thermolysis product | Precursor salt | Ref. |
|--|---------------------|------------------------------------|---------|
| AgSC ₁₂ H ₂₅ | Ag | AgNO ₃ | [23,24] |
| Pd(SC ₁₂ H ₂₅) ₂ | Pd | PdCl ₂ | - |
| Co(SC ₁₂ H ₂₅) ₂ | CoS | Co(OH) ₂ | [25] |
| AuSC ₁₂ H ₂₅ | Au | HAuCl ₄ | [26–28] |
| Co(SC ₁₂ H ₂₅) ₂ | CoS | CoCl ₂ | [25] |
| Pb(SC ₁₂ H ₂₅) ₂ | PbS | Pb(ClO ₄) ₂ | - |
| Cd(SC ₁₂ H ₂₅) ₂ | CdS | Cd(NO ₃) ₂ | [28] |

4. Conclusions

The use of dodecyl-thiolates of transition metals as precursors for the generation of nanoscopic metals and metal sulfides in a molten polymers phase has shown to be a very effective and general approach for the preparation of these materials. Usually, polymeric dispersions of monodisperse nanoparticles are obtained and the nanoparticle size and numerical density can be varied by controlling the amount of dissolved thiolate precursor and the annealing conditions (time and temperature).

References

1. Mayer, A.B.R. Formation of noble metal nanoparticles within a polymeric matrix: Nanoparticle features and overall morphologies. *Mater. Sci. Eng. C* **1998**, *6*, 155–166.
2. Caseri, W. Nanocomposites of polymers and metals or semiconductor: Historical background and optical properties. *Macromol. Rapid Commun.* **2000**, *21*, 705–722.
3. Zimmerman, L.; Weibel, M.; Caseri, W.; Suter, U.W. High refractive index films of polymer nanocomposites. *J. Mater. Res.* **1993**, *8*, 1742–1748.
4. Troger, L.; Hunnefeld, H.; Nunes, S.; Oehring, M.; Fritsch, D. Structural characterization of catalytically active metal clusters in polymer membranes. *Z. Phys. D* **1997**, *40*, 81–83.
5. Gonsalves, K.E.; Carlson, G.; Chen, X.; Kumar, J.; Aranda, F.; Perez, R.; Jose-Yacaman, M. Surface-functionalized nanostructured gold/polymer composite films. *J. Mater. Sci. Lett.* **1996**, *15*, 948–951.
6. Watkins, J.J.; McCarthy, T.J. Polymer/metal nanocomposite synthesis in supercritical CO₂. *Chem. Mater.* **1995**, *7*, 1991–1994.
7. *Chimica Organica Superiore*; Gilman, H., Ed.; Edizioni Scientifiche Einaudi: Torino, Italy, 1956; Volume II, p. 951.
8. Bishop, P.T. The use of gold mercaptides for decorative precious metal applications. *Gold. Bull.* **2002**, *35*, 89–98.
9. Prozorov, T.; Gedanken, A. The “melting point” of alkanethiol-coated amorphous Fe₂O₃ nanoparticles. *Adv. Mater.* **1998**, *10*, 532–535.

10. Rodriguez-Carvajal, J. Recent advances in magnetic structure determination by neutron powder diffraction. *Phys. B* **1993**, *192*, 55–69.
11. Cervellino, A.; Giannini, C.; Guagliardi, A. Determination of nanoparticle, size distribution and lattice parameter from X-ray data for monoatomic materials with f.c.c. cubic unit cell. *J. Appl. Cryst.* **2003**, *36*, 1148–1158.
12. Cervellino, A.; Giannini, C.; Guagliardi, A. Debussy: A Debye user system for nanocrystalline materials. *J. Appl. Cryst.* **2010**, *43*, 1543–1547.
13. Page, K.; Hood, T.C.; Proffen, Th.; Neder, R.B. Building and refining complete nanoparticle structures with total scattering data. *J. Appl. Cryst.* **2011**, *44*, 327–336.
14. *CRC Handbook of Chemistry and Physics*, 82nd ed.; Lide, D.R., Ed.; Chemical Rubber Company: Boca Raton, FL, USA, 2001; pp. 9–51.
15. Nicolais, F.; Carotenuto, G. Synthesis of polymer-embedded metal, semimetal, or sulfide clusters by thermolysis of mercaptide molecules dissolved in polymers. *Rec. Pat. Mater. Sci.* **2008**, *1*, 1–11.
16. Carotenuto, G.; Nicolais, L.; Perlo, P. Synthesis of polymer-embedded noble metal clusters by thermolysis of mercaptides dissolved in polymers. *Polym. Eng. Sci.* **2006**, *46*, 1016–1020.
17. Carotenuto, G.; Nadal, M.L.; Repetto, P.; Perlo, P.; Ambrosio, L.; Nicolais, L. New polymeric additives for allowing photoelectric sensing of plastics during manufacturing. *Adv. Comp. Lett.* **2007**, *16*, 109–114.
18. Capezzuto, F.; Carotenuto, G.; Antolini, F.; Burrese, E.; Palomba, M.; Perlo, P. New fluorescent polymeric nanocomposites synthesized by antimony dodecyl-mercaptide thermolysis in polymer. *eXPRESS Polym. Lett.* **2009**, *3*, 219–225.
19. Carotenuto, G.; Capezzuto, F.; Palomba, M.; Nicolais, F. Synthesis and characterization of fluorescent Cu₂S nanoparticles embedded in amorphous polystyrene, *Int. J. Nanosci.* **2010**, *9*, 385–389.
20. Conte, P.; Carotenuto, G.; Piccolo, A.; Perlo, P.; Nicolais, L. NMR-investigation of the mechanism of silver mercaptide thermolysis in amorphous polystyrene. *J. Mater. Chem.* **2007**, *17*, 201–205.
21. Carotenuto, G.; Longo, A.; DePetrocellis, L.; DeNicola, S.; Repetto, P.; Perlo, P.; Ambrosio, L. Synthesis of molecular gold clusters with luminescence properties by mercaptide thermolysis in polymer matrices. *Int. J. Nanosci.* **2007**, *6*, 65–69.
22. Carotenuto, G.; Hison, C.L.; Capezzuto, F.; Palomba, M.; Perlo, P.; Conte, P. Synthesis and thermoelectric characterization of bismuth nanoparticles. *J. Nanopart. Res.* **2009**, *11*, 1729–1738.
23. Carotenuto, G.; la Peruta, G.; Nicolais, L. Thermo-chromic materials based on polymer-embedded silver clusters. *Sens. Actuat. B* **2006**, *114*, 1092–1095.
24. Carotenuto, G.; Nicolais, F. Reversible thermochromic nanocomposites based on thiolate-capped silver nanoparticles embedded in amorphous polystyrene. *Materials* **2009**, *2*, 1323–1340.
25. Carotenuto, G.; Pasquini, L.; Milella, E.; Pentimalli, M.; Lamanna, R.; Nicolais, L. Preparation and characterization of cobalt-based nanostructured materials. *Eur. Phys. J. B* **2003**, *31*, 545–551.
26. Susa, A.S.; Ringler, M.; Ohlinger, A.; Paderi, M.; Li Pira, N.; Carotenuto, G.; Rogach, A.L.; Feldmann, J. Strongly luminescent films fabricated by thermolysis of gold-thiolate complexes in a polymer matrix. *Chem. Mater.* **2008**, *20*, 6169–6175.

27. Carotenuto, G.; Longo, A.; Hison, C.L. Tuned linear optical properties of gold-polymer nanocomposites. *J. Mater. Chem.* **2009**, *19*, 5744–5750.
28. Carotenuto, G.; Longo, A.; Repetto, P.; Perlo, P.; Ambrosio, L. New polymer additives for photoelectric sensing. *Sens. Actuat. B* **2007**, *125*, 202–206.
29. Carotenuto, G.; Capezzuto, F.; Palomba, M.; Nicolais, F. Synthesis and characterization of fluorescent Cu₂S nanoparticles embedded in amorphous polystyrene. *Int. J. Nanosci.* **2010**, *9*, 1–5.

© 2011 by the authors; licensee MDPI, Basel, Switzerland. This article is an open access article distributed under the terms and conditions of the Creative Commons Attribution license (<http://creativecommons.org/licenses/by/3.0/>).